Technological University Dublin
ARROW@TU Dublin

Articles | School of Electrical and Electronic Engineering

2012

Electrically Tunable Fabry-Perot Resonator Based on Microstructured Sl Contaning Liquid Crystal

V. A. Tolmachev
Ioffe Physico-Technical Institute

V. A. Melnikov
Trinity College Dublin

A. V. Baldycheva
Trinity College Dublin

See next page for additional authors

Follow this and additional works at: https://arrow.tudublin.ie/engscheceart

 Part of the Electrical and Electronics Commons

Recommended Citation

Tolmachev, V.A., Melnikov, V.A. ,Baldycheva, A.V., Berwick, K., Perova, T.S. (2012) Electrically tunable fabry-perot resonator based on microstructured si containing liquid crystal. *Progress In Electromagnetics Research*, Vol. 122, 293-309, 2012. doi:10.2528/PIER11091506

This Article is brought to you for free and open access by the School of Electrical and Electronic Engineering at ARROW@TU Dublin. It has been accepted for inclusion in Articles by an authorized administrator of ARROW@TU Dublin. For more information, please contact arrow.admin@tudublin.ie, aisling.coyne@tudublin.ie.

This work is licensed under a Creative Commons Attribution-Noncommercial-Share Alike 4.0 License
Funder: IRCSET, Ireland Postdoctoral Award, the ICGEE Postgraduate Programme and by the Science Foundation Ireland (NAP-94 Programme).

Authors
V. A. Tolmachev, V. A. Melnikov, A. V. Baldycheva, Kevin Berwick, and T. S. Perova

This article is available at ARROW@TU Dublin: https://arrow.tudublin.ie/engscheceart/148

Progress In Electromagnetics Research, Vol. 122, 293–309, 2012

ELECTRICALLY TUNABLE FABRY-PÉROT RESONATOR BASED ON MICROSTRUCTURED SI CONTAINING LIQUID CRYSTAL

V. A. Tolmachev[1], V. A. Melnikov[2, 4], A. V. Baldycheva[2], K. Berwick[3], and T. S. Perova[2, *]

[1]Ioffe Physical Technical Institute, Polytechnicheskaya 26, St.-Petersburg, Russia

[2]Department of Electronic and Electrical Engineering, Trinity College Dublin, Dublin 2, Ireland

[3]School of Electronic and Communications Engineering, Dublin Institute of Technology, Kevin St, Dublin 8, Ireland

[4]Division of Physical Sciences and Engineering, 4700 King Abdullah University of Science and Technology, Thuwal 23955-6900, Kingdom of Saudi Arabia

Abstract—We have built Fabry-Pérot resonators based on microstructured silicon and a liquid crystal. The devices exhibit tuning of the resonance peaks over a wide range, with relative spectral shifts of up to $\Delta\lambda/\lambda = 10\%$. In order to achieve this substantial spectral shift, cavity peaks of high order were used. Under applied voltages of up to 15 V, a variation in the refractive index of the nematic liquid crystal E7 from $\Delta n_{\mathrm{LC}} = 0.12$ to $\Delta n_{\mathrm{LC}} = 0.17$ was observed. These results may have practical applications in the near-, mid and far-infrared range.

1. INTRODUCTION

Silicon photonics [1] allows integration of optical and electronic functions on the same die, enabling low-cost manufacturing and fast data transfer. Devices based on optical microcavities can be used in a wide range of applications [2]. One example is the Fabry-Pérot (FP) resonator, which consists of a pair of parallel mirrors with a cavity between them [3]. Incorporating an electro-optic material into the microcavity with a large birefringence Δn, such as a Liquid Crystal

Received 15 September 2011, Accepted 10 November 2011, Scheduled 21 November 2011

* Corresponding author: Tatiana S. Perova (perovat@tcd.ie).

(LC) [4], allows structures with tunable photonic properties to be fabricated. These devices are fabricated using porous Si layers of different porosities or thin, multilayer coatings and the direction of propagation of light is perpendicular to the substrate [5]. One of the most effective ways of tuning the optical properties of the material within the cavity is by applying an electric field. For the nematic liquid crystal E7, with $\Delta n \approx 0.2$, relative shifts in the resonant frequency, expressed as a percentage, of up to $\Delta\lambda/\lambda = 1.1\%$ in Ref. [6] and $\Delta\lambda/\lambda = 8\%$ in Refs. [7, 8] have been observed. These, as well as other recent investigations, have demonstrated the possibility of electro-tuning in LC-FP resonators.

For integrated silicon microphotonics, the preferred direction of light propagation is parallel to the substrate, requiring microstructuring of the semiconductor substrate. A device of this type, based on a cavity introduced into a two-dimensional (2D) photonic crystal (PC) was suggested in Ref. [9], where the reorientation of the LC and a consequent relative shift of the resonance peak of up to $\Delta\lambda/\lambda = 0.5\%$ were achieved using an applied voltage of 10 V. In paper [10], it is demonstrated that an FP resonator can be obtained by fabricating only two microstructured Si walls, the mirrors, with an air gap, the resonant cavity, between them. This cavity can be infiltrated with an LC.

A schematic diagram of this type of resonator is shown in Fig. 1(a). Due to the high optical contrast of Si/LC, the calculated reflection coefficient, R, in the stop-band maximum may reach 0.95. The transmission coefficient, T, can vary from 0.05 to 1. A large spectral shift in the high order resonance modes was demonstrated by varying the refractive index, n, of the medium in the resonator

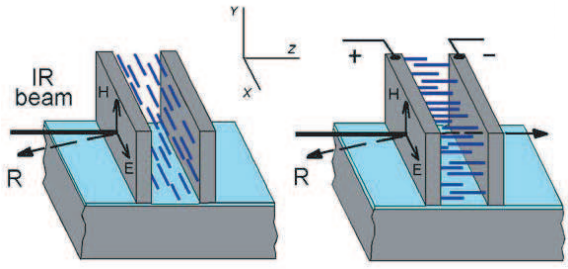

Figure 1. Schematic diagram of the Fabry-Pérot resonator, consisting of two Si walls separated by a gap infiltrated with liquid crystal molecules with (a) horizontal planar and (b) homeotropic alignment.

cavity [10]. Despite the simplicity of this design, electrotuning of the resonant modes in this type of FP-resonator, filled with LC E7, was experimentally demonstrated, with relative shifts of up to $\Delta\lambda/\lambda = 3.2\%$.

In this study, an LC-FP resonator with an optimized design, based on a combination of reflection and transmission gap maps, was fabricated. A detailed investigation of electrotuning of the device is described. The device exhibits a large shift in the resonant peaks and a reversible tuning of the high-order resonant peaks as a result of the LC transition from planar (Fig. 1(a)) to homeotropic alignment (Fig. 1(b)).

2. CALCULATIONS

In order to design an optimal structure for Fabry-Pérot resonators, we use maps of the Photonic Band Gaps (PBGs) or Stop Bands (SBs) [11, 12]. In order to draw the map of the SBs for a 1.5-period photonic crystal, considered here as an FP-resonator, we generate values of the filling fraction of Si, f_{Si}, from 0 to 1, with a step size of 0.01, assuming that the parameter $a = d_{cav} + d_{Si}$ is constant, and $f_{Si} = d_{Si}/a$.

Then, using the Transfer Matrix Method (TMM) [13], a set of R spectra, ~ 100 in total, are calculated for values of f_{Si} varying from 0 to 1 at a normal incidence of light. The incoming and outcoming medium was air, with $n = 1$. We use a refractive index for Si of $n_{Si} = 3.42$ [14], and extreme values of the ordinary (n_o) and extraordinary (n_e) refractive indices (Fig. 2(a), insert) of the liquid crystal E7 with n_{LC} equal to 1.49 and 1.69, respectively, in the mid-IR [15] range. Values of the reflection coefficient, R, above a particular cut off [16, 17], chosen here to be $R_{cutoff} > 0.85$, are plotted on the graph versus normalized frequency, $NF = a/\lambda$, as shown in Fig. 2(a). This, lower than usual, value for the cut off criterion for SBs of $R_{cutoff} = 0.85$ is chosen for clarity.

As shown in Fig. 2(a), the oval SB regions obtained are relatively wide, due to the high optical contrast and the low value of R_{cutoff} used. The SB regions for the resonator with $n_{\mathrm{LC}} = 1.69$ are red shifted with respect to the SBs for the resonator with $n_{\mathrm{LC}} = 1.49$. The relative shift, $\Delta NF/NF$, is substantial, over a range of $f_{Si} = 0.02$–0.2 and for values of $NF \sim 1$, for example, (see Fig. 2(b)). It can also be seen from this figure that the SB regions are shifted by an amount equal to their total width as a result of the variation of n_{LC} from 1.49 to 1.69.

In order to identify regions with high transparency, the set of calculated R spectra for f_{Si} values from 0 to 1 is filtered using

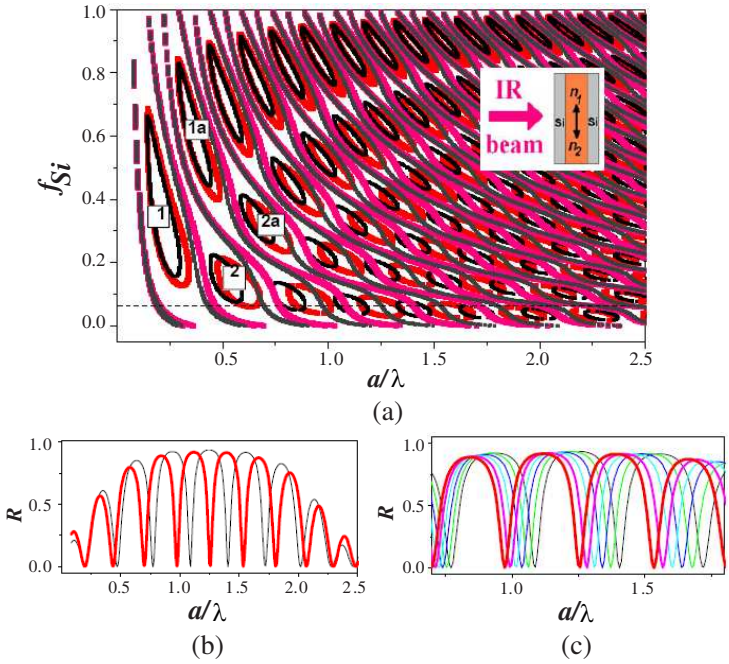

Figure 2. (a) Map of stop-bands (oval-like areas) and transmission bands (shown by lines) for a 1.5-period PC (FP-resonator) based on a 3-layer "Si-LC-Si" model with two values of $n_{\mathrm{LC}} = 1.49$ (thick contour) and 1.69 (thin contour). $R_{cutoff} = 0.85$, $T_{cutoff} = 0.99$. (b) Spectrum R calculated for $f_{Si} = 0.06$ (see dotted line in figure (a)) used for drawing the SBs map. (c) Fine tuning of peak positions and stop-bands with variation of n_{LC} from 1.49 ($n_1 = n_o$) to 1.69 ($n_2 = n_e$) with a step size of $\Delta n = 0.04$. The relative peak shift $\Delta NF/NF = 10.5\%$.

a different cut off criterion of $R_{cutoff} < 0.01$, which is equivalent to the condition $T_{cutoff} > 0.99$. This procedure allows a map of the transmission bands, (TBs) [18], or pass-bands, to be plotted on the previously obtained map of the SBs. This allows a clearer demonstration of the location of the transmission bands with respect to the SBs, as a function of f_{Si} (Fig. 2(a)). In the TB regions, resonant modes with high signal modulation ($\Delta T = T_{\max} - T_{\min} \approx 0.95$) as well as low signal modulation are included [19]. Consequently, the TB region must be surrounded by two stop-bands on the gap map. For example, for $f_{Si} = 0.5$ and 0.3 in Fig. 2(a), there are no closely spaced SBs around the TB regions, between the regions 1-1a and 1-2a respectively, and, therefore, the corresponding resonance peaks do

not possess a high signal modulation. This effect is obvious to an even greater extent in the spectra shown in Fig. 2(b). These spectra demonstrate that a variation in n of 0.2 in the resonant cavity leads to a shift of the resonance peak, for example, from 1.40 to 1.26 *NF,* a relative shift of $\Delta NF/NF = 0.14/1.33 = 10.5\%$. The width of the stop-band in this case is $\sim 0.2NF$, and the SBs are shifted by approximately half their width as a result of tuning. Obviously, the LC molecules can be oriented so that their refractive index is at an intermediate value between n_o and n_e. Fig. 2(c) depicts the spectra for these intermediate values of n_{LC}, demonstrating the possibility of fine tuning both the resonant peaks and the position of the stop-bands.

The simulations presented in Fig. 2(a) demonstrate that the relative shift of the resonance peak in the region of SBs 1 and 2 is minimal, while in the high order stop-bands, a substantial change in the position of the resonant peaks can be expected. The calculations are performed using normalized frequency units, $NF = a/\lambda$, so they are applicable to any wavelength range. When selecting an FP-resonator it is necessary to consider both the maximum possible shift of the resonance peaks that can be obtained as well as the maximum value of spectral modulation, i.e. the difference between the maximum and minimum value of R in the spectra — ideally $\Delta R = |R_{\max}–R_{\min}| \sim$ 0.95–0.99. Clearly, a structure with a large LC component would be expected to have a stronger influence, via its refractive index, on the resonance peaks positions. So, in order to experimentally verify the simulation results, FP resonators with filling fractions of $f_{\mathrm{LC}} \sim 0.8$ and ~ 0.9, or $f_{Si} \sim 0.2$ and ~ 0.1, respectively, were used.

3. EXPERIMENT

The FP resonator was fabricated using optical lithography and anisotropic etching of (110) Silicon-On-Insulator (SOI) wafers. Anisotropic chemical etching was used for microstructuring the (110) Si [20], because this technology generates high quality, 'mirror-like' Si side-walls and, therefore, excellent infrared spectra. Thermally grown silicon dioxide was used as a mask when etching the wafers. The thickness of the Si device layer and the Buried Oxide (BOX) layer were 20 µm and 2 µm, respectively. The choice of 20 µm for the depth, in particular, was dictated by the minimum size of the IR microscope aperture used for optical characterization, in conjunction with an FTIR, FTS 6000 spectrometer [21]. A view of a typical resonator, fabricated on (110) Si, is depicted in Fig. 3. The cavity was infiltrated with commercial LC E7 (Merck) [22] using a specially designed reservoir and the channels shown in Fig. 3. Si wall-electrodes

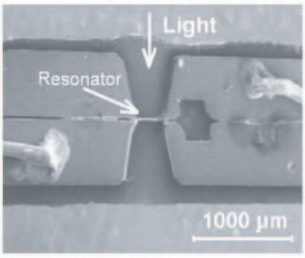

Figure 3. SEM image of the top view of the FP resonator fabricated on an SOI wafer.

were connected to the outer pads by attaching thin metal wires to the chip contact areas with conductive silver paste. An AC rectangular pulse train, with various amplitudes between 0.5 V and 15 V, with a pulse duration of $\tau_p = 1$ ms and a frequency of $f_p = 100$ Hz was used to drive the device [23].

Optical characterisation was performed with a polarized FTIR microspectrometer in reflection, R, and transmittance, T, modes in the wavenumber range of $\nu = 650$–$6500\,\mathrm{cm}^{-1}$ ($\lambda = 1.5$–$15\,\mu$m). For polarized infrared measurements, the electric vector of the incident light is aligned with the Si grooves for E-polarized light, while for H-polarized light the electric vector is aligned along the depth direction of the grooves as shown in Fig. 1(a).

A best fit to the experimentally registered spectra using simulated spectra calculated using the Transfer Matrix Method [13] was performed. For the empty resonator ($n_{cav} = 1$) the fit was performed with a Si wall width of $d_{Si} \approx 1 \pm 0.3\,\mu$m and a cavity width of $d_{cav} \approx 4.0 \pm 0.3\,\mu$m as fitting parameters, while for the LC FP resonator, n_{cav} was used as a fitting parameter. The characteristic vibrational bands of the liquid crystal were also analysed, together with the interference bands of high reflection, the Stop Bands, and the resonant transmission peaks. Note that all the experimental spectra (R and T) are presented in this paper in arbitrary, or normalized, units in order to clearly compare the results. Normalization of the data was necessary due, in particular, to a shading effect [21] of the focused light beam onto the Si wall of the resonator, integrated onto the chip, during infrared measurements.

Reflection spectra in E- and H-polarization, registered from a $20 \times 20\,\mu\mathrm{m}^2$ area of an FP LC-resonator prior to the application of the electric field are shown in Fig. 4(a). A pronounced shift of the interference bands in the reflection spectra as a result of the change in the polarization of the probe beam from E to H-polarization is

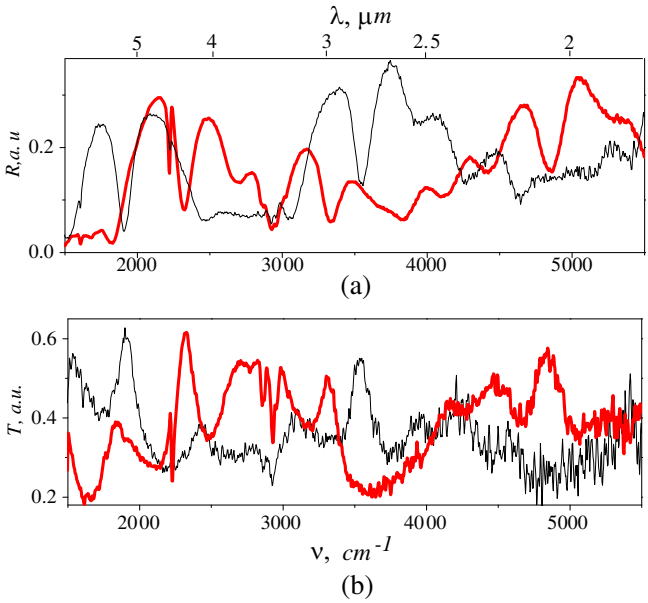

Figure 4. FTIR (a) Reflection and (b) Transmission spectra of the FP resonator with LC filler for E (thick line) and H (thin line) polarizations in the absence of an applied electric field. The resonator parameters are: width of Si walls, $d_{Si} = 1\,\mu$m, cavity width, $d_{cav} = 4\,\mu$m.

observed, confirming the anisotropy of the LC molecules infiltrated into the resonator. In other words, this shift is caused by the alignment of the LC director along some preferred orientation within a Si groove and, therefore, due to the influence of the ordinary, n_o, and extraordinary, n_e, refractive indices for the appropriate polarization. Similar results are obtained from the same spot when measuring the transmission, T, spectra (Fig. 4(b)). We note that the transmission spectra are noisier than those taken in reflection, due to the reduction in the total intensity of the light transmitted through the resonator. Nevertheless, general trends in the behavior of reflection and transmission spectra are clearly seen from a comparison of Figs. 4(a) and 4(b). For both polarizations, the position of the minima in the transmission spectra corresponds to the maxima of the reflection spectra and *vice versa*.

A fit to the R spectra from the LC FP resonator results in a value of $n_{cav} = 1.57$ for E-polarization, and $n_{cav} = 1.45$ for H-polarization, using known values of $d_{Si} = 1\,\mu$m and $d_{cav} = 4\,\mu$m. The value of $n_{cav} = 1.45$ for H polarization obtained appears to be smaller than

the value of $n_o = 1.49$ from the literature for LC E7 [15]. This discrepancy will be discussed in the following section. The presence of the LC in the cavity is confirmed by observation of the absorption band of LC E7 molecules at $2222\,\mathrm{cm}^{-1}$ [24] in the R (Fig. 4(a)) as well as in the T (Fig. 4(b)) spectra for E-polarization. Two other intense absorption bands of LC E7, which could have been used for the analysis of the orientation of LC molecules, are typically observed at 1497 and $1602\,\mathrm{cm}^{-1}$ [24]. In Fig. 4, they are near the minima of the interference bands and are hidden. So, only the vibrational band at $2222\,\mathrm{cm}^{-1}$ was utilised in this case. We note that for the H-spectrum, this band is suppressed significantly in comparison to the E-spectrum. This behavior is typical of the dichroism of LC molecules. The dominant behavior of the band at $2222\,\mathrm{cm}^{-1}$ for E-polarized spectra indicates a preferred orientation of the LC director in the X-direction, along the groove, as shown in Fig. 1(a).

Under an applied voltage of 10 V, the E-spectra are blue-shifted, as seen in Figs. 5(a) and 5(c), indicating that the value of n_{LC} is reduced in the resonator by the electric field. The H-spectra are practically unchanged by the electric field (not shown). The intensity of the vibrational band of the LC at $2222\,\mathrm{cm}^{-1}$ is decreased in the E-spectrum at 10 V (Figs. 5(a) and 5(c)), indicating that a reorientation of molecules from the initial, planar, alignment to homeotropic alignment has occurred, in accordance with the model presented in Figs. 1(a) and 1(b). The value of $n_{cav} = 1.45$ (at 10 V) obtained appears to be lower in this case than the $n_{cav} = 1.57$ previously observed at 0 V in the E-polarized spectrum. In the former case, the orientation of the LC is driven by the electric field and would be strongly expected to be homeotropic. In accordance with the schematic shown in Fig. 1(b), for homeotropic alignment of LC molecules, n_{cav} must correspond to the refractive index, n_o, of LC E7, i.e., to be equal to 1.49. The value obtained by us from the fitting routine of 1.45 is smaller than 1.49 by 0.04. This deviation is larger than any inaccuracies that you would expect from determining the value of n from the fitting routine, which would typically be $\delta n = \pm 0.02$.

As already noted, after infiltration of the LC into FP resonator, the value of n_{cav} was determined to be 1.57 for the E-spectrum (at 0 V). This value is close to the expected refractive index value for a random orientation of the LC molecules $n_{rand} = 1.56$ [15]. However, dichroism, clearly observed for the $2222\,\mathrm{cm}^{-1}$ absorption band, indicated that the initial orientation of LC molecules was planar. In this case, from the literature, n_e must be equal to 1.69 [15], while from the fit of the spectra a significantly smaller value, of $n_{\mathrm{LC}} = 1.57$, was obtained.

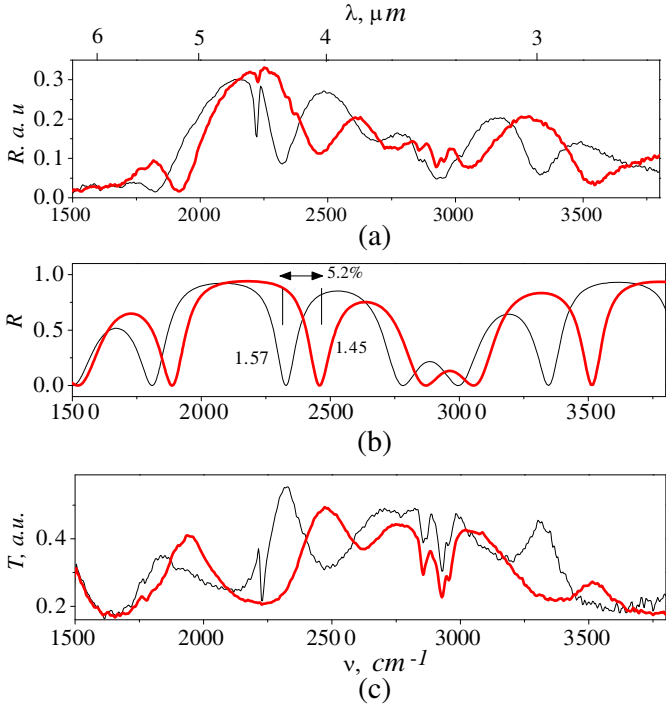

Figure 5. Experimental (a) Reflection and (c) Transmission spectra in E-polarization in the absence (0 V — thin line) and presence (10 V thick line) of an applied electric field. The spectral shift observed demonstrates the reorientation of LC molecules in the FP cavity from planar to homeotropic alignment. (b) Calculated reflection spectra, obtained from the best fit, for two values of n_{cav} shown beside the curves. Resonance peaks are seen at 1800, 2320 and 3400 cm^{-1}, corresponding to 5.6, 4.2 and 2.9 μm.

Therefore we conclude from the spectral fitting process that both of the calculated n values (n_o and n_e) are smaller than those predicted by the model.

One possible reason for the lower values of n_{LC} could be the presence of air voids inside the groove with LC. Indeed, air voids are visible in some SEM images of our LC infiltrated devices. In order to avoid the appearance of air voids, it is better to perform the infiltration of the LC at higher temperatures, typically at the temperature of the isotropic phase. However, in this study, the infiltration of the LC was intentionally carried out at room temperature, where the LC E7 is in the nematic phase. In our experience, infiltration

under these conditions results in a spontaneous planar orientation of the LC director, either along the depth or along the length of the grooves [25]. In our experiment, the degree of infiltration of LC in the groove is normally observed using an optical microscope, allowing the propagation of the LC molecules along the groove, the X direction in Fig. 1(a), and the infiltration quality to be assessed.

The results obtained using the Effective Medium Approach [26] indicate the possibility of the existence of a volume fraction of air voids in the cavity of $V_{air} = 0.08$, i.e., 8% [10]. This explains the lower values of n obtained from fitting the experimental spectra for both E and H polarizations.

The spectrum registered across the whole infrared range, as well as the spectrum in the region of the vibrational mode at 2222 cm^{-1}, reverts to that originally seen at 0 V on removal of the electric field. Therefore, in this work, we have demonstrated, for the first time, a spontaneous planar orientation of nematic LC molecules on an untreated Si surface, which can be reversed by the removal of the electric field, using voltages up to 10 V. As a result of electrotuning, these FP peaks are shifted reversibly by 128, 168 and 206 cm^{-1}, corresponding to relative shifts of $\Delta\lambda/\lambda = 4.2$, 5.2 and 4.8%.

We also investigated the resonant peak shifts at intermediate applied voltages of between 0 V and 10 V, as demonstrated in Fig. 6 for E-polarization in the spectral range from 3000–3800 cm^{-1}. The applied voltage of 1.5 V is not enough to cause reorientation of the LC

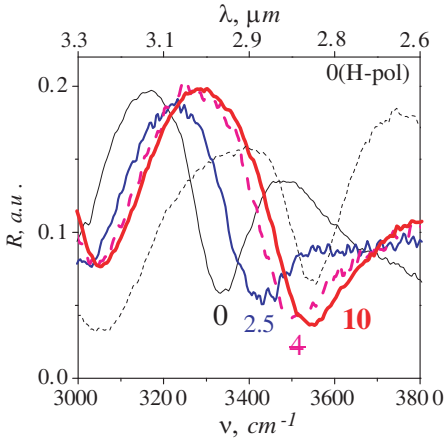

Figure 6. Smooth tuning of the position of the resonance peak from 3330 cm^{-1} to 3550 cm^{-1} for E- and H-polarization (dotted line). The applied voltage is shown in volts beside each curve.

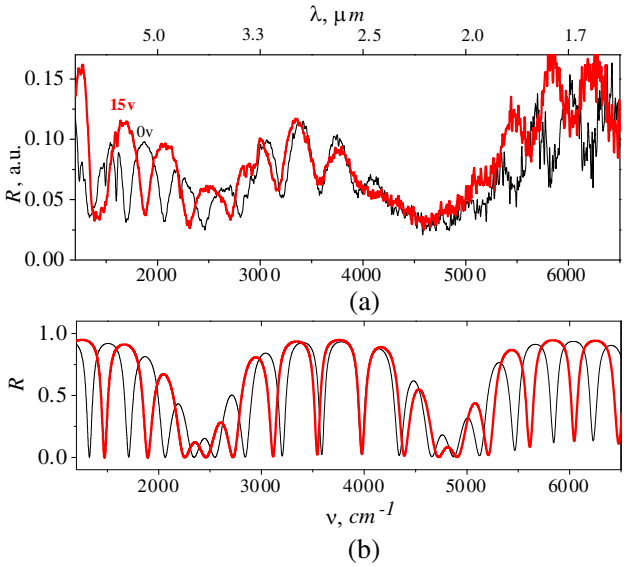

Figure 7. (a) Experimental and (b) calculated E-polarized spectra of the FP resonator with $d_{Si} = 0.6\,\mu\text{m}$ and $d_{cav} = 7.4\,\mu\text{m}$ without electric field (thin line) and with an electric field generated by an applied voltage of 15 V (thick line). Application of a voltage of 15 V results in a shift of the resonance peaks across the spectral range. The best fit, shown in Fig. 7(b), is obtained at $\Delta n_{\text{LC}} = 0.17$ ($n_{\text{LC}} = 1.51$, 0 V)) and ($n_{\text{LC}} = 1.34$, 15 V).

from one state to another. At 2.5 V, which is close to the threshold voltage of LC E7 (1.5 V), a pronounced shift of the bands is seen. The shift reaches a maximal value at a voltage of 10 V. We note that the position of the resonance peak at 10 V for E-polarization corresponds to the position of this peak at 0 V for H-polarization, as expected from the alignment models demonstrated in Figs. 1(a) and 1(b).

A similar experiment was conducted on a different sample with a higher filling fraction of $f_{\text{LC}} \approx 0.9$ ($f_{Si} \approx 0.1$). By fitting the experimental spectrum for the empty sample, a value of $d_{Si} = 0.6\,\mu\text{m}$ was obtained, with a resonator cavity width, $d_{cav} = 7.4\,\mu\text{m}$ ($f_{Si} = 0.07$). The reflection spectrum, registered for this sample after LC infiltration, shows that the band positions shift, depending on the polarization of the probe beam, that is, the system exhibits anisotropy. For E-spectrum of R (Fig. 7(a)), all three characteristic vibrational bands of the LC (at 1497, 1602 and 2222 cm^{-1}) have a higher intensity than those in the same spectrum taken using H-polarization (not

shown). This indicates that an orientation of the LC molecules along the X-axis has occurred (Fig. 1(a)). Reflection spectra in E-polarization, registered after electric field application, are shown in Fig. 7(a). The applied voltage of 15 V results in a blue-shift of the E-spectrum, and to a decrease in the intensity of the LC peaks, as demonstrated previously, causing a homeotropic orientation of the LC molecules (Fig. 1(b)). The results of the best fit to the experimental spectra, using n_{LC} as a fitting parameter and values of $d_{Si} = 0.6\,\mu\mathrm{m}$ and $d_{cav} = 7.4\,\mu\mathrm{m}$, are presented in Fig. 7(b). The characteristic FP peaks are seen in the calculated spectrum, which coincide well with the relevant experimental peaks across the spectral range investigated from 650 to 6500 cm^{-1} (see Fig. 7(a)). The shifts in the experimental spectrum obtained after the application of an electric field are also present in the simulated spectrum. In addition, after the application of a voltage of 15 V, the intensity of all three vibrational bands of the LC decreases significantly, confirming the transition of the LC to a homeotropic alignment.

The electro-optical effect observed here can be considered reversible, because after the electric field was switched off (0 V) the spectrum returns to its initial state, corresponding to a planar orientation of the LC molecules. The same effect was observed in the first sample. Fig. 8 shows intermediate spectra, obtained using a range of applied voltages from 0 V to 15 V, in an extended spectral region from 1480 to 2300 cm^{-1}. These spectra demonstrate the possibility of fine tuning the resonance peaks. This tuning effect is clearly apparent in, for example, the vicinity of $\sim 1750\,\mathrm{cm}^{-1}$ ($\lambda = 5.7\,\mu\mathrm{m}$).

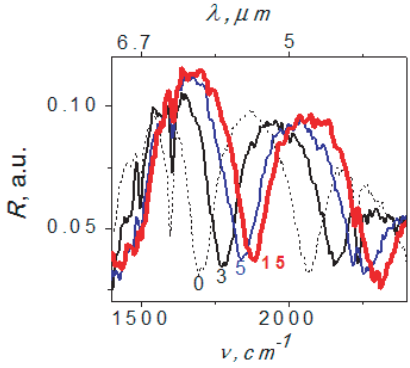

Figure 8. Smooth tuning of the resonance peak from 1700 to 1880 cm^{-1} in the experimental reflection spectra of the FP resonator (from Fig. 5) with a maximal relative shift of $\Delta\lambda/\lambda = 10\%$.

The reorientation of LC molecules under an applied voltage is also clearly demonstrated by the change in intensity of the $1602\,\mathrm{cm}^{-1}$ vibrational band. As noted earlier, the values obtained for the parameter n_{LC}, calculated during the fitting routine, are slightly lower than the ordinary and extraordinary refractive indices of LC E7 from the literature. Note that the values of birefringence of 0.12 and 0.17 are close to the $\Delta n_{LC} = 0.2$ obtained for LC E7 in the mid-IR range [15]. We assume that the lower n_{LC} values obtained here are related to the presence of a small number of voids in the LC, created during the LC infiltration process.

4. RESULTS ANALYSIS

An electrotunable LC FP resonator, based on the principle of changing the optical thickness of the LC resonator, using resonance peaks of high order [10], has been demonstrated in this investigation. This electro-optical device is based on microstructured silicon with LC filler. To the best of our knowledge, the closest existing analogue to the device suggested is a hybrid photonic crystal microcavity switch, as described in Ref. [9]. In this device, a relative shift in the resonance mode of the order of $(\Delta\lambda/\lambda) = 0.5\%$ in the near infrared range was achieved as a result of the electro-optical effect obtained due to the reorientation of LC E7 in the cavity of a two-dimensional photonic crystal. We would also like to mention Ref. [27], where a shift of the resonance peak of $(\lambda/\lambda) = 0.5\%$ was reported, due to a variation in the geometrical thickness of the FP air cavity driven by an electric field applied to the second movable mirror. Therefore, the FP resonator demonstrated in our work, fabricated by microstructuring of Si, is significantly better than comparable devices, given that the resonant peak shift varied from 5% to 10%. This can be explained by the fact that i) we use the resonance peaks in the stop bands of high order, where a significant shift of the consequent defect mode can be obtained as a result of the change in Δn in the electro-optical material used and ii) in comparison with the rough interface in a 2D microcavity, the application of an LC with plane-parallel reflectors provides the most effective distribution of "switchable" molecules with respect to the Si side-walls and the applied electric field. We demonstrated the optical properties of this type of LC FP-resonator in the mid-infrared range, enabling us to simultaneously analyse the behaviour of the LC E7 vibrational modes. Investigations of the optical properties of electro-optical devices in the mid-IR range are also technologically important. Si-LC composite materials, and switchable elements based on them, are being researched aggressively, due to their transparency in this spectral range and these devices

may have application in biochemical sensing, medicine, defense and security [28].

Finally, we note that the demonstrated electrotunable model of Fabry-Perot resonator can be applied to the realization of any one-dimensional photonic micro- and nano-devices such as tunable bandpass filters [29, 30], photonic crystal mirrors [31, 32], polarizers [33], polarizing beam splitters [34, 35], channel-drop filters [36] and multichanneled filters [37] for application in the wide electro-magnetic spectral range.

5. CONCLUSION

A Fabry-Pérot resonator, consisting of two silicon walls, also acting as electrodes, and a thick cavity, filled with the nematic liquid crystal E7, was fabricated on a Si-On-Insulator platform. The Reflection and Transmission spectra of this resonator were investigated using Fourier Transform Infrared microspectroscopy, in the spectral range from 650 to 6500 cm^{-1} (1.5 to 15 μm). The spectra obtained are in good agreement with the results of calculations based on the Transfer Matrix Method and Gap Map Method. In particular, a superposition of the transmission peaks with reflection maxima, predicted from calculations, was confirmed experimentally. Altering the liquid crystal alignment, and consequently the refractive index value in the cavity, by the application of an electric field using voltages from 0 V to 15 V, results in reversible tuning of the high-order resonance peaks with relative shifts of up to $\Delta\lambda/\lambda \approx 10\%$.

ACKNOWLEDGMENT

This work has been supported by the IRCSET, Ireland Postdoctoral Award, the ICGEE Postgraduate Programme and by the Science Foundation Ireland (NAP-94 Programme). Support from the Russian Foundation for Basic Research 09-02-00782, is also gratefully acknowledged. The authors wish to express their appreciation to G. Fedulova for help with sample fabrication, and A. V. Astrova for useful discussions.

REFERENCES

1. Jalali, B. and S. Fathpour, "Silicon photonics," *J. of Lightwave Techn.*, Vol. 24, No. 12, 4600–4615, 2006.
2. Vahala, K. J., "Optical microcavities," *Nature*, Vol. 424, 839–846, 2003.

3. Kaklamani, D. I., "Full-wave analysis of a Fabry-Perot type resonator," *Progress In Electromagnetics Research*, Vol. 24, 279–310, 1999.
4. Busch, K. and S. John, "Liquid-crystal photonic-band-gap materials: The tunable electromagnetic vacuum," *Phys. Rev. Lett.*, Vol. 83, No. 5, 967–970, 1999.
5. Ghulinyan, M., C. J. Oton, G. Bonetti, Z. Gaburro, and L. Pavesi, "Free-standing porous silicon single and multiple optical cavities," *J. Appl. Phys.*, Vol. 93, No. 12, 9724, 2003.
6. Weiss, S. M. and P. M. Faushet, "Electrically porous silicon active mirrors," *Phys. Stat. Sol. (a)*, Vol. 197, No. 2, 556–560, 2003.
7. Ozaki, R., T. Matsui, M. Ozaki, and K. Yoshino, "Optical property of electro-tunable defect mode in 1D periodic structure with (liquid) crystal defect layer," *Electronics and Communications in Japan*, Part 2, Vol. 87, No. 5, 24–31, 2004.
8. Pucker, G., A. Mezzetti, M. Crivellari, P. Belluti, A. Lui, N. Daldosso, and L. Pavesi, "Silicon-based near-infrared tunable filters filled with positive or negative dielectric anisotropic liquid crystals," *J. Appl. Phys.* Vol. 95, 767–769, 2004.
9. Anderson, S. P., M. Haurylau, J. Zhang, and P. M. Fauchet, "Hybrid photonic crystal microcavity switches on SOI," *Proc. SPIE*, Vol. 6477, 647712-1/8, 2007.
10. Tolmachev, V. A., V. A. Melnikov, V. Baldycheva, T. S. Perova, and G. I. Fedulova, "Design, fabrication and optical characterization of Fabry-Pérot tunable resonator based on microstructured Si and liquid crystal," *Proc. SPIE*, Vol. 7713, 771320-1, 2010.
11. Joannopoulos, J. D., R. D. Meade, and R. D. Winn, *Photonic Crystals*, 184, Princeton University Press, 1995.
12. Joannopoulos, J. D., S. G. Winn, and R. D. Meade, *Photonic Crystals. Molding the Flow of Light*, 2nd Edition, Princeton University Press, 2008.
13. Azzam, R. M. A. and N. M. Bashara, *Ellipsometry and Polarized Light*, 334, Amsterdam, North-Holland, 1977.
14. Palik, E. D., *Handbook of Optical Constants of Solids*, Academic Press, 1998.
15. Khoo, L. C., "The infrared optical nonlinearities of nematic liquid crystals and novel two-wave mixing processes," *J. Mod. Opt.*, Vol. 37, No. 11, 1801–1813, 1990.

16. Tolmachev, V. A., T. S. Perova, and K. Berwick, "Design criteria and optical characteristics of one-dimensional photonic crystals based on periodically grooved silicon," *Appl. Opt.*, Vol. 42, 56–79, 2003.
17. Tolmachev, V., T. Perova, E. Krutkova, and E. Khokhlova, "Elaboration of the gap map method for the design and analysis of one-dimensional photonic crystal structures," *Physica E: Low-dimensional Systems and Nanostructures*, Vol. 41, 1122–1126, 2009.
18. Baldycheva, A., T. Perova, and V. Tolmachev, "Formation of infrared regions of transparency in one-dimensional silicon photonic crystals," *IEEE Photonics Technology Letters*, Vol. 23 No. 4, 200–202, 2011.
19. Tolmachev, V. A., T. S. Perova, and A. Baldycheva, "Transformation of one-dimensional silicon photonic crystal into Fabry-Pérot resonator," *Proc. SPIE*, Vol. 7943, 79430E-1, 2011.
20. Tolmachev, V. A., E. V. Astrova, J. A. Pilyugina, T. S. Perova, R. A. Moore, and J. K. Vij, "1D photonic crystal fabricated by wet etching of silicon," *Optical Materials*, Vol. 27, No. 5, 831–835, 2005.
21. Tolmachev, V. A., T. S. Perova, E. V. Astrova, B. Z. Volchek, and J. K. Vij, "Vertically etched silicon as 1D photonic crystal," *Phys. Stat. Solidi (a)*, Vol. 197, No. 2, 544–549, 2003.
22. Data Sheet Licristal®E7, Merck KGaA, Germany, 2001.
23. Tolmachev, V. A., S. A. Grudinkin, J. A. Zharova, V. A. Melnikov, E. V. Astrova, and T. S. Perova, "Electro-tuning of the photonic band gap in SOI-based structures infiltrated with liquid crystal," *Proc. SPIE*, Vol. 6996, 69961Z, 2008.
24. Wu, S., U. Efron, and L. V. D. Hess, "Infrared birefringence of liquid crystals," *App. Phys. Lett.*, Vol. 44, No. 11, 1033–1035, 1984.
25. Perova, T. S., V. A. Tolmachev, and E. V. Astrova, "Tunable photonic structures based on silicon and liquid crystals (Invited)," *Proc. SPIE*, Vol. 6801, 68010W, 2008.
26. Bruggeman, D. A. G., "Berechung verschiedener physikalisher Konstanten von heterogenen Substanzen," *Ann. Phys.*, Vol. 24, 636–664, Leipzig, 1935.
27. Lipson A. and E. M. Yeatman, "A 1-D photonic band gap tunable optical filter in (110) silicon," *J. of Microelectromechanical Systems*, Vol. 16, No. 3, 521–527, 2007.

28. Soref, R., "Mid-infrared photonics in silicon and germanium," *Nature Photonics*, Vol. 4, 495–497, 2010.
29. Smolyakov, A. I., E. A. Fourkal, S. I. Krasheninnikov, and N. Sternberg, "Resonant modes and resonant transmission in multi-layer structures," *Progress In Electromagnetics Research*, Vol. 107, 293–314, 2010.
30. Ni, J., B. Chen, S. L. Zheng, X.-M. Zhang, X.-F. Jin, and N. Chi, "Ultra-wideband on electrooptic phase modulator and phase-shift fiber Bragg grating," *Journal of Electromagnetic Waves and Applications*, Vol. 24, No. 5–6, 795–802, 2010.
31. Manzanares-Martinez, J., R. Archuleta-Garcia, P. Castro-Garay, D. Moctezuma-Enriquez, and E. Urrutia-Banuelos, "One-dimensional photonic heterostructure with broadband omnidirectional reflection," *Progress In Electromagnetics Research*, Vol. 111, 105–117, 2011.
32. Wu, C.-J., Y.-C. Hsieh, and H.-T. Hsu, "Tunable photonic band gap in a doped semiconductor photonic crystal in near infrared region," *Progress In Electromagnetics Research*, Vol. 114, 271–283, 2011.
33. Khalaj-Amirhosseini, M. and S. M. J. Razavi, "Wide-angle reflection wave polarizers using inhomogeneous planar layers," *Progress In Electromagnetics Research M*, Vol. 9, 9–20, 2009.
34. Liu, Y. and Z. Lu, "Phase shift defect modes in one-dimensional asymmetrical photonic structures consisting of two rugate segments with different periodicities," *Progress In Electromagnetics Research*, Vol. 112, 257–272, 2011.
35. Wu, C.-J., J.-J. Liao, and T.-W. Chang, "Tunable multilayer Fabry-Perot resonator using electro-optical defect layer," *Journal of Electromagnetic Waves and Applications*, Vol. 24, No. 4, 531–542, 2010.
36. Shchegolkov, D. Y., C. E. Heath, and E. I. Simakov, "Low loss metal diplexer and combiner based on a photonic band gap channel-drop filter at 109 GHz," *Progress In Electromagnetics Research*, Vol. 111, 197–212, 2011.
37. Hsu, H.-T., M.-H. Lee, T.-J. Yang, Y.-C. Wang, and C.-J. Wu, "A multichanneled filter in a photonic crystal containing coupled defects," *Progress In Electromagnetics Research*, Vol. 117, 379–392, 2011.